Deformation of partially molten granite: A review and comparison of experimental and natural case studies

Article *in* International Journal of Earth Sciences · January 2001

DOI: 10.1007/s005310000164

CITATIONS
108

READS
386

1 author:

Claudio Rosenberg
Sorbonne Université
88 PUBLICATIONS **3,161** CITATIONS

SEE PROFILE

Int J Earth Sciences (Geol Rundsch) (2001) 90:60–76
DOI 10.1007/s005310000164

ORIGINAL PAPER

Claudio L. Rosenberg

Deformation of partially molten granite: a review and comparison of experimental and natural case studies

Received: 1 November 1999 / Accepted: 9 October 2000 / Published online: 6 March 2001

Abstract Experimental and natural investigations of partially molten granite are compared and reviewed. Experiments suggest that deformation of partially molten granite with low-viscosity melt (10^4 Pa s) exhibits a rheological critical melt percentage (RCMP). In case of high viscosity melts (10^8 Pa s), however, the relationship between melt fraction and log viscosity of the partially molten granite may be linear. Considerations about viscosity, rheological thresholds, and segregation of natural melts suggest that low-viscosity melt experiments simulate natural conditions more realistically. Therefore, an RCMP is to be expected under natural conditions. Both diffusion creep and dislocation creep may occur under natural conditions, whereas cataclastic flow is only observed under experimental conditions. A melt-induced transition from dislocation creep to diffusion creep occurs under experimental and natural conditions. Melt topology is controlled by the magnitude of differential stress under experimental conditions. If differential stress is higher than ~100–150 MPa, melt pockets are elongate and oriented at a low angle to the maximum compressive stress. In contrast, in nature, melt pockets tend to be oriented subparallel to the foliation plane, i.e., presumably at a high angle to the maximum compressive stress.

Keywords Granite · Melt · Melt topology · Synmagmatic deformation · Experimental deformation · Magmatic microstructure

C.L. Rosenberg (✉)
Fachrichtung Allgemeine Geologie, Freie Universität Berlin, Malteserstrasse 74–100, 12249 Berlin, Germany
E-mail: cla@zedat.fu-berlin.de
Phone: +49-30-83870902
Fax: +49-30-7759078

Introduction

Seismic data indicate that large portions of the middle crust of orogenic belts are partially molten (e.g., Nelson et al. 1996; Schmitz and Kley 1997). It is often suggested that melt weakens the crust, thus inducing large-scale localization of deformation and decoupling (e.g., Hollister and Crawford 1986; Handy 1990). Hollister and Crawford (1986) showed that areas of rapid uplift are bounded by crustal-scale, melt-bearing shear zones, and they introduced the concept of melt-enhanced deformation. Many examples have been described from transpressive (e.g., Davidson et al. 1992) and transcurrent (e.g., Vauchez and Egydio da Silva 1992) crustal-scale shear zones, where melts are spatially and temporally associated with localised deformation. The notion of melt-enhanced deformation is intuitively sound, and offers a satisfying interpretation of some isothermal decompression paths described in many high-temperature mylonitic belts (Hollister and Crawford, 1986). However, little is known about the physical processes underlying melt-enhanced deformation. Lubrication, which was suggested by Hollister and Crawford (1986) to induce this process, may not be important, because deformation deep in the crust, even in the presence of melt, mainly occurs by viscous flow, i.e., in the absence of friction (see also discussion in Dell'Angelo and Tullis 1988).

Many experiments performed over the past 20 years, concerning deformation of both crustal and mantle rocks in the presence of low melt fractions (<0.25) showed that melting induces several changes in the mechanical behaviour of the material. First, several melt-induced transitions were documented in both dominant and accommodating deformation mechanisms: from dislocation creep to fracturing (Dell'Angelo and Tullis 1988), from dislocation creep to diffusion creep (Cooper and Kohlstedt 1984; Dell'Angelo et al; 1987), and from dislocation creep

to dislocation creep involving grain boundary sliding (Hirth and Kohlstedt 1995b). Second, melt induces changes in the spatial distribution of deformation. Rosenberg and Handy (2000) showed that the onset of melting in a deforming analogue aggregate corresponds to the transition from distributed deformation to localized deformation along shear bands. Third, melting induces important volume and pore pressure changes in the deforming rock, thus varying its strength.

Whereas melt modifies the mechanical behavior of rocks, deformation modifies the flow direction and distribution of melt in partially molten rocks (e.g., Daines and Kohlstedt 1997), thus controlling melt segregation pathways and the seismic properties of partially molten crust. Depending on the experimental conditions, deformation can induce melt segregation (Dell'Angelo and Tullis 1988) or conversely, the sucking of melt into the deforming and dilating region (van der Molen and Paterson 1979).

Investigations of granitic rocks naturally deformed in the presence of melt allow us to evaluate whether microstructures and melt geometries resulting from experiments reproduce those in nature. Melt distributions are well-described on the outcrop scale (for example, leucosomes in migmatites), but little is known about melt geometry on the grain scale. A large number of studies on the microstructures of partially molten crustal rocks has focussed on the reaction textures and paragenesis of these rocks. Only few studies tried to infer the deformation mechanisms and melt distribution on the basis of microstructural criteria. These studies will be reviewed below.

Several reviews have been published recently on the deformation of partially molten crustal rocks. Rushmer (1996); Rutter (1997) and Brown and Rushmer (1997) reviewed the results of experimental deformation of partially molten rocks, focusing on related segregation processes. Sawyer (1999) reviewed criteria for the identification of microstructures formed during partial melting under both static and dynamic conditions. Finally, Vernon (2000) reviewed microstructural criteria to distinguish magmatic from solid-state flow. In the present study I will compare the results of experimental and field investigations on the deformation of partially molten granite. The points of discrepancy and agreements between these two areas of research will be outlined. Although in this paper I deal primarily with granite, I will also refer to the literature on partially molten mantle rocks, since mantle rocks have been studied in greater detail than has granite. In addition, I will use knowledge from "see-through" deformation experiments (e.g., Means 1989) on partially molten analogue materials to constrain processes that cannot always be inferred from thin sections of samples quenched after deformation.

Experimental deformation of partially molten granite

The first deformation experiments performed on partially molten granite (Murrel and Chakravarty 1973; Murrel and Ismail 1976) showed that incipient melting dramatically reduces the strength of the aggregate. The melt fraction in these experiments was poorly determined (<0.25) and it was only at the end of the 1970s that new experiments constrained the strength of the sample as a function of melt fraction (Arzi 1978; van der Molen and Paterson 1979). These investigations led to the concept of a rheological critical melt percentage (RCMP), a restricted range of melt fractions (between 0.1 and 0.3) in which "most of the viscosity drop from that of the full solid to that of the full melt occurs" (Arzi 1978). This concept, which is discussed in detail in the following paragraph, has strongly influenced ideas on the rheology of partially molten rocks (e.g., Marsh 1981; Gapais and Barbarin 1986; Wickham 1987; Nicolas 1992; Fernandez and Gasquet 1994; Holtz et al. 1996, Berger and Kalt 1999), the interpretation of synmagmatic fabrics (e.g., Gapais and Barbarin 1986; Paterson et al. 1998), and more recently the thermal modelling of crystallizing granitic mushes (Barboza and Bergantz 1998).

The concept of RCMP

Arzi (1978) performed deformation experiments using partially molten granite containing melt fractions up to 0.17. The viscosity of the samples decreased by two orders of magnitude when the melt fraction increased from 0.12 to 0.17. In addition, the strength reduction became more pronounced with increasing melt content, as shown by the steepening of the melt fraction vs. viscosity curve towards higher melt fractions (Fig. 1). On the same diagram, Arzi (1978) plotted the Einstein-Roscoe relationship (Roscoe 1952) for melt fractions ≥ 0.5 (Fig. 1). He suggested that the region delimited between the steepening of his experimental curve and the vertical segment of Roscoe's curve corresponds to the transition between a flow regime controlled by the solid component of the aggregate to a flow regime controlled by the melt. Arzi (1978) termed this transition the RCMP and suggested that it would occur between melt fractions of 0.1 and 0.3.

Van der Molen and Paterson (1979) performed a series of experiments under similar conditions to those of Arzi (1978), and also observed a dramatic decrease in strength with increasing melt content. The point of maximum rate of strength reduction, i.e., the inflection point of the viscosity vs. melt fraction curve of Fig. 1, was suggested to correspond to a melt fraction of 0.3 to 0.35. This value was termed the critical melt fraction (CMF). Note however that the CMF was not experimentally defined. The low melt fractions used in these experiments and those of Arzi (1978) could only

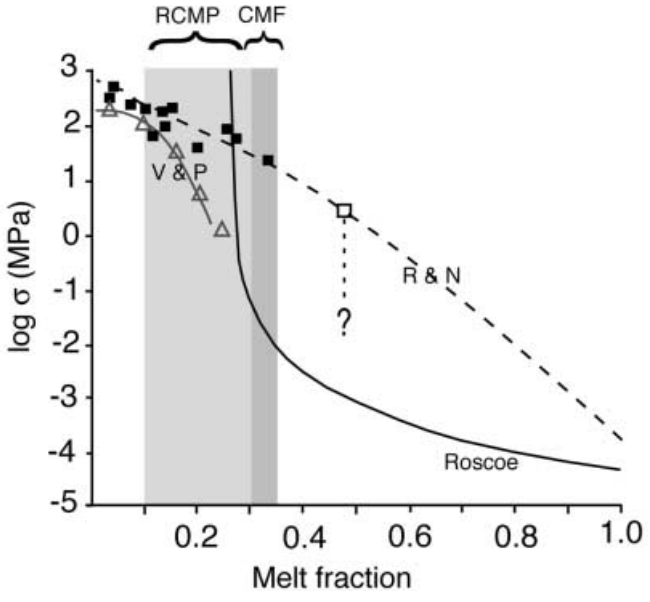

Fig. 1 Melt fraction vs. log strength diagram, modified from Rutter and Neumann (1995). *Open triangles* van der Molen and Paterson (1979), *solid squares* Rutter and Neumann (1995), *open square* experiment of Rutter and Neumann (1995), in which sample strength was too low to be measured. *Solid curve* Roscoe's equation solved for a melt viscosity of 10^4 Pa s. Roscoe's equation was formulated to describe the flow of solutions containing different amounts of solid particles $\eta=\eta_0 (1.35\phi\text{-}0.35)^{-2.5}$, where η is the viscosity of the bulk aggregate (melt + crystals), η_0 is the viscosity of the melt and ϕ is the crystal fraction

constrain the lower boundary of the RCMP (Fig. 1). The upper boundary of the RCMP was estimated by semi-empirical laws that describe the viscosity of suspensions at different solid fractions (Roscoe 1952; Jeffrey and Acrivos 1976). Roscoe's equation, which approximates these empirical laws, yields a curve which asymptotically approaches an infinite viscosity when the melt fraction tends to 0.26 (Fig. 1). By combining this curve with the experimentally derived one for granite, Arzi (1978) postulated a sigmoidal curve to illustrate the change in viscosity of granite over its entire range of melting. The same was done by van der Molen and Paterson (1979), but using the equation of Jeffrey and Acrivos (1976). The validity of Roscoe's equation to describe the rheological behaviour of partially molten silicates is strengthened by the experiments of Lejeune and Richet (1995), whose results perfectly coincide with Roscoe's equation in the range of melt fractions between 1 and 0.4. However, a deviation from Roscoe's equation has also been reported from experiments on partially molten granite (Bagdassarov and Dorfman1998). This deviation is probably due to the asperity of the quartz grains used in the experiments.

Recently, Rutter and Neumann (1995) reinvestigated the mechanical behaviour of partially molten granite as a function of melt fraction. They performed experiments up to melt fractions of 0.45 at strain rates and confining pressure similar to those applied by Arzi (1978) and van der Molen and Paterson (1979). In contrast to the previous experiments, Rutter and Neumann (1995) did not vary the melt content of their samples by adding different amounts of water. Instead, they used dry samples and varied the temperature between 800 and 1,100 °C, thereby inducing melt fractions from 0.03 to 0.5. They found a linear relationship between melt fraction and log. viscosity (Fig. 1) and no evidence for an RCMP. Note, however, that the strength of the sample containing 0.48 melt plotted in Fig. 1 represents the maximum possible strength of that sample. The absolute strength is unknown, because the very low differential stresses supported by the granite at such high melt content is below the range of reliable measurements. If the absolute strength of this sample is assumed to be lower, e.g., as low as the question mark plotted in Fig. 1 by Rutter and Neumann (1995), the relationship between log. viscosity and melt fraction results in a curve with an inflection point at approximately 0.4 melt fraction. This suggests the existence of an RCMP, even though it is at higher melt fractions and is less pronounced than previously thought. Rutter and Neumann (1995) conclude that the occurrence of the RCMP in previous experiments is due to the water added to the samples in order to decrease the melting temperature. In fact, water markedly reduces the viscosity of the melt (e.g., Holtz et al. 1996), hence also of the bulk aggregate.

The absence of an RCMP in the experiments of Rutter and Neumann (1995) is alternatively interpreted (Renner et al. 2000), as due to dilatancy hardening (Brace and Martin 1968). This effect results from dilatancy prior to fracturing, which reduces the pore pressure and hence increases the strength of the rock. For highly viscous fluids, this effect is more pronounced, because the time needed to reequilibrate the pore pressure perturbation by melt flow is longer. The effect of dilatancy hardening balances the weakening that results from the increasing melt fraction, masking the RCMP. In contrast, the lower viscosity of the melt (10^4 Pa s) in the experiments of Arzi (1978) and van der Molen and Paterson (1979) allows a rapid reequilibration of the pore pressure changes, hence minimizing the effect of dilatancy hardening.

Additional insight into the RCMP concept may be gained from the experiments of Lejeune and Richet (1995) performed in a piston cell with silicate melt of garnet pyrope composition at room confining pressure and 0.3 to 1 melt fractions. These experiments clearly show the existence of an RCMP, but at higher melt fractions (0.4–0.6) than found by Arzi (1978) and van der Molen and Paterson (1979). Moreover, Lejeune and Richet (1995) experimentally constrained the "upper boundary" of the RCMP at melt fractions of 0.6. Dilatancy hardening could not develop in these experiments due to the lack of confining pressure.

In summary, whether or not the RCMP occurs in experimentally deformed partially molten granite

depends on the experimental conditions. Deformation at high strain rates with high viscosity melts may result in a nearly linear relationship between strength and melt fraction. Instead, for lower melt viscosities, the relationship between strength and melt fraction is not linear and characterized by an RCMP.

Is the RCMP present in nature?

In order to answer the question on the occurrence of the RCMP in nature, I will summarize some of the observations and inferences made on natural magmatic rocks that are relevant to the concept of the RCMP:

1. The water content of natural granitic melts is expected to be between 3 and 7% (Scaillet et al. 1997) and the viscosity to be rather constant and approximately $10^{4.5}$ Pa s (Scaillet et al. 1998) or 10^3 to 10^6 Pa s (Clemens and Petford 1999). Therefore, experiments exhibiting an RCMP, performed with added water and thus low viscosity melts, may reflect natural conditions more adequately.
2. Lava flows commonly have a maximum crystal fraction of 0.6 (Wada 1995; Scaillet et al. 1998), exceptionally 0.65 (Wyborn et al. 1981; Wickham 1987), irrespective of their composition. These values were interpreted to reflect a major rheological transition, where further flow is inhibited because magma viscosity increases dramatically at melt fractions smaller than 0.4 (Marsh 1981). A similar conclusion can be drawn from the observation that the crystal fraction in the centre of lava conduits, where the shear rate is at its minimum, does not exceed 0.5 to 0.7 (Komar 1972). In lavas, an RCMP may therefore occur at melt fractions of 0.3 to 0.5.
3. Syntectonic melt segregation may be so effective that a melt fraction larger than 0.1 is never reached in the anatectic protolith (Brown and Rushmer 1997). It may be concluded that the RCMP hardly occurs in migmatites. However, this statement does not take into account the possible heterogeneous distribution of the melt (see Smith 1997 for a review of natural case studies). Analogue experiments (Rosenberg and Handy 2000) show that melt-bearing shear bands containing melt fractions higher than those of the bulk aggregate (Fig. 2) interconnect during deformation. In this case, an RCMP may occur, when melt-bearing shear bands interconnect.
4. Dilatancy hardening may well occur under laboratory conditions at high strain rates (10^{-3} to 10^{-4} s^{-1}). However, it is unlikely to occur under natural strain rates, except during seismic events (Brace and Martin 1968). As a consequence, the masking effect that dilatancy hardening may have on the RCMP is not expected to occur under natural conditions.
5. The RCMP is observed in experiments performed under brittle conditions (Arzi 1978, van der Molen and Paterson 1979). In contrast, viscous-type of deformation mechanisms control the flow of partially molten granite under natural conditions (Rosenberg and Riller 2000). If the experiments were also conducted in the viscous regime, the strength of the rocks at low melt fractions (0.0 to 0.1) would be smaller than that found under brittle conditions. Therefore, the strength drop at the RCMP may be less pronounced under natural conditions (see also Barboza and Bergantz 1998). In contrast, van der

Fig. 2 Micrograph (plane light) of a quenched sample of norcamphor deformed in the presence of melt by simple shear. Simple shear experiment performed in a Means-Urai "see-through" deformation apparatus. Average melt percentage is 10–15%. *Upper* and *lower side* of the picture correspond to the shear zone boundary. The quenched melt is *dark gray*. It is distributed along grain boundaries, melt-bearing shear bands (*C′*, delimited by *half arrows*) containing ~30% melt, and in the matrix (between the shear bands), containing <10% melt. Melt is preferentially located along grain boundaries oriented subparallel to the incremental shortening direction ε_3 (*full arrows* point to such grain boundaries). *Full arrowheads* indicate a melt-bearing bridge interconnecting two shear bands. *Black points* are corundum particles that were used as strain markers

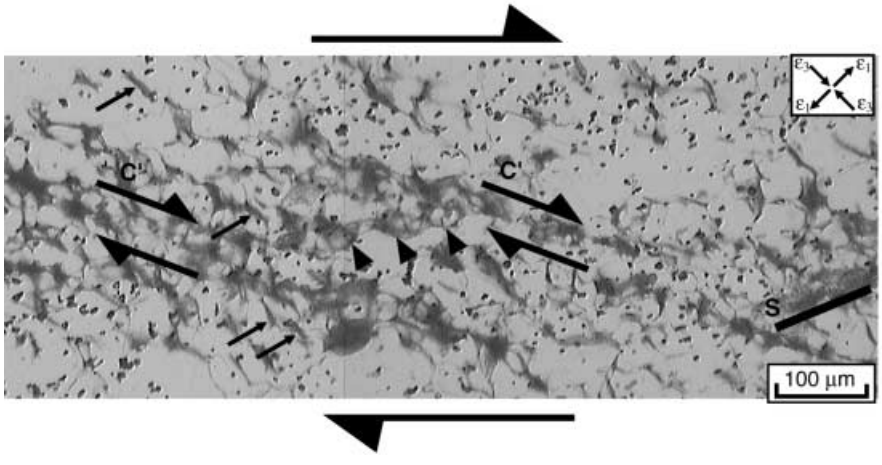

Molen and Paterson (1979) suggest that the general form of the viscosity vs. strength curve should not vary as a function of deformation mechanisms operating at low melt fractions. The strength variation due to a change in the dominant deformation mechanism (e.g., dislocation creep vs. diffusion creep) is probably not significant compared with the strength drop of several orders of magnitude associated with the attainment of the RCMP.

Deformation mechanisms in partially molten granite

Fracturing

Most laboratory deformations of partially molten granitic rocks resulted in cataclastic flow (Arzi 1978; van der Molen and Paterson 1979; Paquet and François 1980; Auer et al. 1981; Paquet et al. 1981; Dell'Angelo and Tullis 1988; Rutter and Neumann 1995). Rutter (1997) pointed out that the occurrence of brittle behaviour at such high temperatures is due to the low confining pressure of the experiments (<400 MPa), impeding the onset of intracrystalline plasticity in quartz and feldspar. This interpretation is supported by the occurrence of dislocation creep only in experiments conducted at confining pressures $\geq$1.0 GPa (Dell'Angelo et al. 1987; Dell'Angelo and Tullis 1988; Gleason et al. 1999). Note that if the melt is interconnected, the experiments may be considered as unconfined, irrespective of the applied confining pressure, due to the pore pressure effect of the melt (Renner et al. 2000). Another reason for cataclastic flow is the large grain size (mostly between 0.3 and 1 mm) of the natural samples used for the experiments, which suppresses diffusion-accommodated mechanisms at laboratory strain rates.

Dislocation and diffusion creep

Dell'Angelo et al. (1987) and Dell'Angelo and Tullis (1988) performed their experiments at confining pressures of 1.5 GPa. In addition, they used fine-grained (<10 μm) synthetic quartz-feldspar mixtures to facilitate deformation in the diffusion-creep regime. These experiments demonstrate that the occurrence of melt fractions as small as 0.05 induces fracturing in a rock that, in the absence of melt but at the same pressure, temperature and strain rate conditions, would otherwise flow by dislocation creep assisted by dynamic recrystallization (Fig. 3). If grain sizes are sufficiently small (<10 μm), diffusion creep replaces dislocation creep as the dominant deformation mechanism for melt fractions as small as 0.03 to 0.05, as previously shown for olivine aggregates in the presence of basaltic melt (Cooper and Kohlstedt 1984). These melt-induced transitions in the deformation mechanisms illustrate two fundamental properties of melts. First, melt behaves like a fluid and creates a pore pressure that reduces the effective strength of the rock, eventually leading to fracturing. Second, melt enhances diffusion rates, and hence facilitates the grain shape readjustments needed to accommodate grain-boundary sliding.

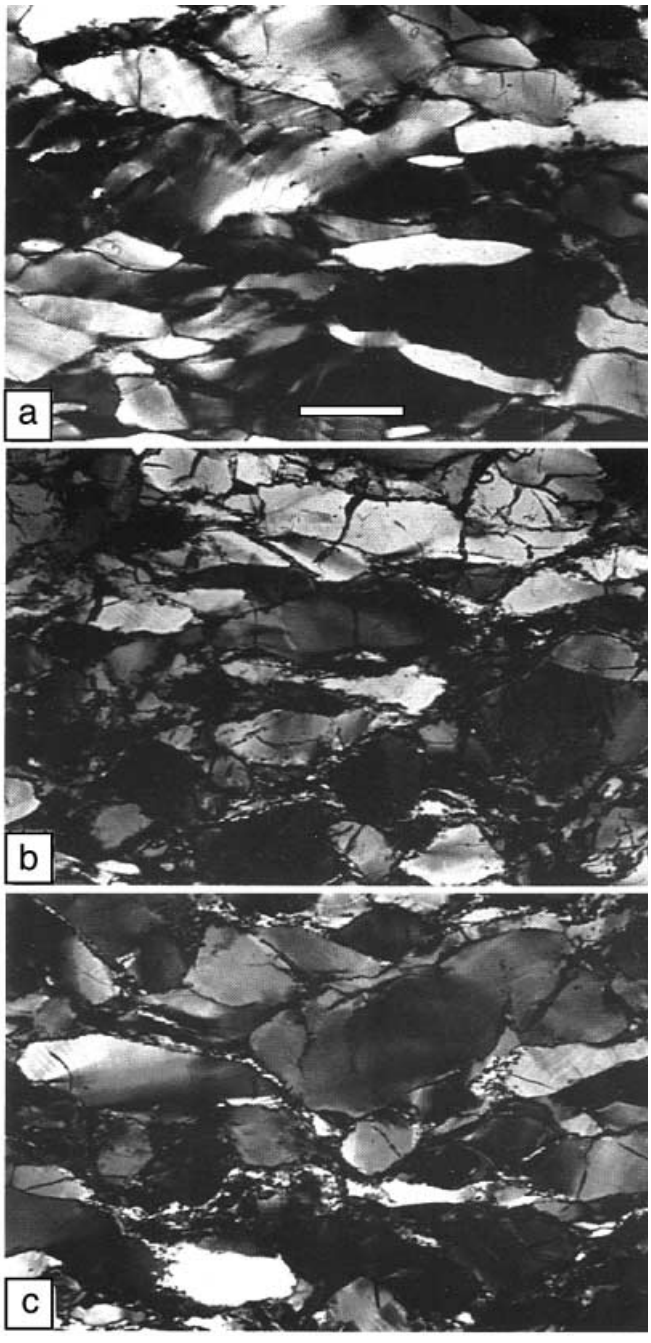

Fig. 3a–c Micrographs of aplite samples, experimentally deformed at a strain rate of 10^{-6} s^{-1}, 900 °C, and 1,500 MPa (reproduced from Dell'Angelo and Tullis 1988). *Scale bar* is 100 μm. Shortening direction is vertical. **a** No melt. Grains are internally deformed and elongated parallel to the plane of flattening. **b** 5% melt. Grains are flattened, but also recrystallized along their margins. In addition, grains are dissected by fractures subparallel to the shortening direction. **c** 10% melt. Greater amount of fine-grained recrystallized material and cracks

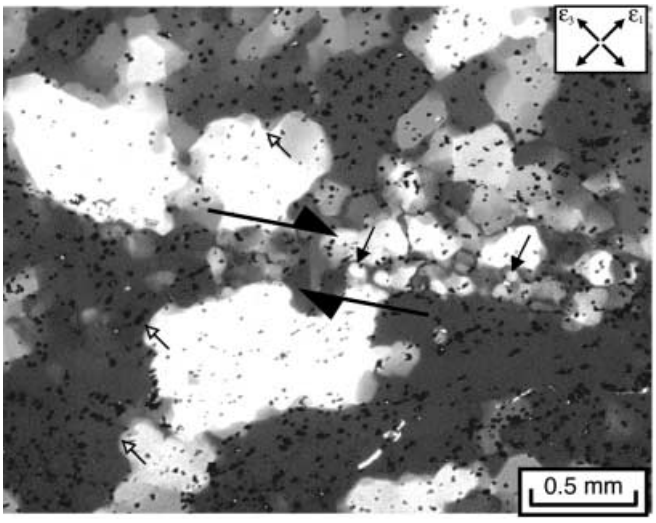

Fig. 4 Micrograph (crossed polarizers) of norcamphor in the presence of melt deformed by simple shear in a "see-through" deformation apparatus. The sample contains 10–15% melt, not visible in this micrograph, distributed along grain boundaries. Melt distribution from a similar experiment can be observed in the plane light micrograph of the quenched sample of Fig. 2. Deformation within the shear bands takes place by diffusion-accommodated grain boundary sliding (Rosenberg and Handy 2000). Note the pronounced grain size reduction tracing the dextral shear band (*half arrows*). In the matrix outside of the shear band deformation takes place by dislocation creep involving dynamic recrystallization, and minor intergranular fracturing. *Black dots* are corundum particles that were used as strain markers. *Solid arrows* point to small, rounded and isotropic grains. *Open arrows* point to lobate grain boundaries, indicating dynamic recrystallization outside of the shear band

The transition from dislocation creep to diffusion creep was also documented in "see-through" deformation experiments performed on partially molten analogue materials (Rosenberg and Handy 2000). In these experiments, a mixture of norcamphor and benzamide, used to simulate quartz and feldspar, respectively, was sheared at a strain rate of 8×10^{-5} s^{-1} in the presence of a norcamphor-benzamide eutectic melt up to a melt fraction of ~0.1. These experiments documented a strain-induced transition from distributed deformation by dislocation creep, involving dynamic recrystallization and intergranular fracturing, to localized deformation by diffusion creep along interconnected, melt-bearing shear bands (Figs. 2 and 4). In contrast to the findings by Dell'Angelo et al. (1987), the onset of diffusion-creep was not achieved by reducing the grain size of the samples previous to deformation. Instead, grain size reduction occurred during deformation within areas of strain localization (shear bands), mainly as a result of melting.

Grain boundary sliding

This mechanism has often been inferred to control or participate in the deformation of partially molten rocks. On the basis of mechanical data, Jin et al. (1994) and Hirth and Kohlstedt (1995b) inferred the occurrence of grain boundary sliding during experimental deformation of partially molten mantle rocks in the dislocation creep regime. Park and Means (1997) showed that grain- and phase-boundary sliding were the dominant mechanisms during their "see-through" deformation experiments on partially molten analogue materials. Sliding of grains past each other was evidenced by comparison of pictures taken at different time intervals. In addition, the experiments of Park (1994) and Park and Means (1996, 1997) cast a new light on the processes accommodating grain boundary sliding. Experiments conducted at slow strain rates (10^{-6} s^{-1}) over a wide range of melt fractions (between 0.5 and 0.05) during crystallization, showed that deformation was partly accommodated by dissolution at grain-to-grain contacts (Fig. 5b, c). Comparison of images taken at different strain increments indicated that crystallizing, euhedral grains were shortened by dissolution at grain-to-grain contacts. This process was termed "contact melting" by the authors.

The effect of melt on the onset of grain boundary sliding is also documented during "see-through" deformation experiments of norcamphor in the presence of melt (Fig. 6). Melt intrudes along intergranular fractures, subparallel to the shortening direction (Fig. 6b, c), and sliding of grains occurs locally, only along these melt-coated grain boundaries (Fig. 6c). These experiments suggest that grain boundary sliding accommodated by diffusion or intracrystalline plasticity is strongly favored by the presence of melt. This mechanism is difficult to identify due to the lack of diagnostic microstructures, but may be the prime mode of deformation of granite in the presence of melt.

Recrystallization mechanisms in partially molten granite

The effect of melt on dynamic recrystallization in granite is poorly known. Dell'Angelo and Tullis (1988) showed that higher melt fractions up to 0.1 enhance dynamic recrystallization of quartz and feldspar. However, it is not clear whether this effect should be ascribed to the presence of melt or to the water added to the samples to induce the melting reaction. Indeed, water is known to enhance dynamic recrystallization (e.g., Urai 1983).

Deformation experiments on partially molten mantle rocks are controversial in this respect. Whereas Jin et al. (1994) and Bai et al. (1997) observed that melt enhances dynamic recrystallization, Hirth and Kohlstedt (1995b) noted that melt inhibits recrystallization. Own experiments using norcamphor (Rosenberg and Handy, in review) show that melt-free grain-boundaries of aggregates deformed in the dislocation creep regime are very mobile. In contrast, grain boundaries

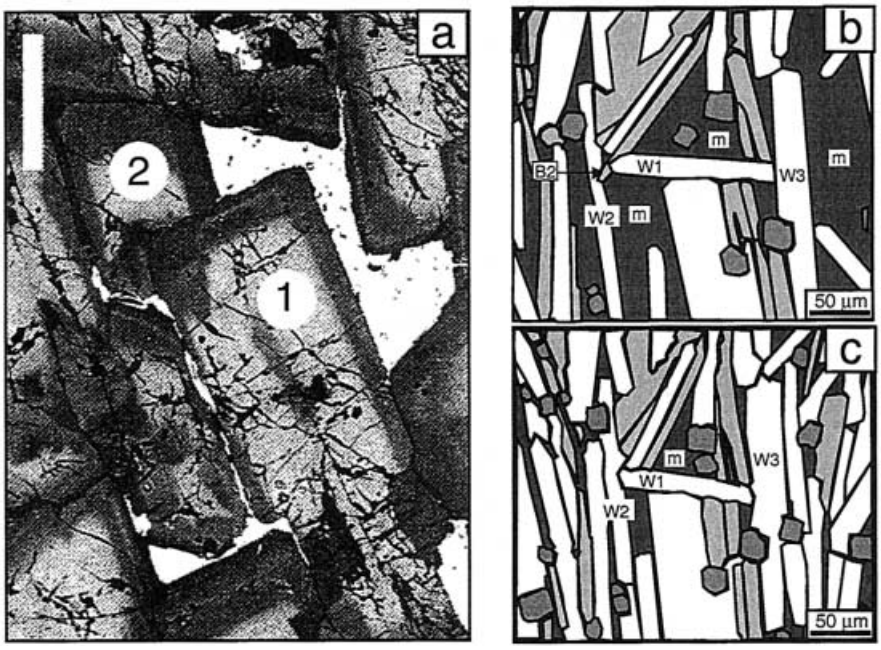

Fig. 5a–c Natural and experimental examples of deformation by contact melting. **a** Gabbro of the Oman Ophiolite (reproduced from Nicolas and Ildefonse 1996, Geophysical Research Letters). Note impingement of plagioclase 1 into plagioclase 2, strongly suggesting dissolution of their outer zonation rims. *Scale bar* is 0.5 mm. **b**, **c** Experimentally deformed partially molten analogue materials, redrawn from Park and Means (1996). Two stages of the synkinematic crystallization of a crystal mush are illustrated. *Dark gray* is the melt (*m*). *Lighter grays and white grains* represent three crystal phases crystallizing from a eutectic melt. Note that grains B2 and W1 are shortened during crystallization of the aggregate, in the absence of crystal plastic strain and recrystallization. This feature was interpreted as resulting from contact melting. *Field width* 0.3 mm

coated with melt in the same aggregate are stable (Fig. 6). Intergranular melt films in these experiments have widths of 10–50 µm and are therefore too large to allow the migration of a grain boundary into a neighboring grain. This interpretation is consistent with the postulation of Urai et al. (1986) of enhanced grain boundary migration velocities in the presence of a thin intergranular fluid film, and inhibited grain boundary migration for large fluid-film thicknesses.

Fig. 6 Pure shear deformation of norcamphor in the presence of melt in a Means-Urai "see-through" deformation rig. Microstructural sequence showing how the shape and distribution of melt pockets change during progressive deformation. *Dark gray* melt-bearing intergranular fractures, *light gray* melt pockets resulting from static melting of previous benzamide grains and parts of the host grains of norcamphor, *stippled lines* subgrain boundaries, *small open spots* corundum particles that serve as strain markers. *Large numbers* refer to melt pockets, *small numbers* refer to strain markers. *Half arrows* relative displacements by grain boundary sliding. Shortening direction is vertical

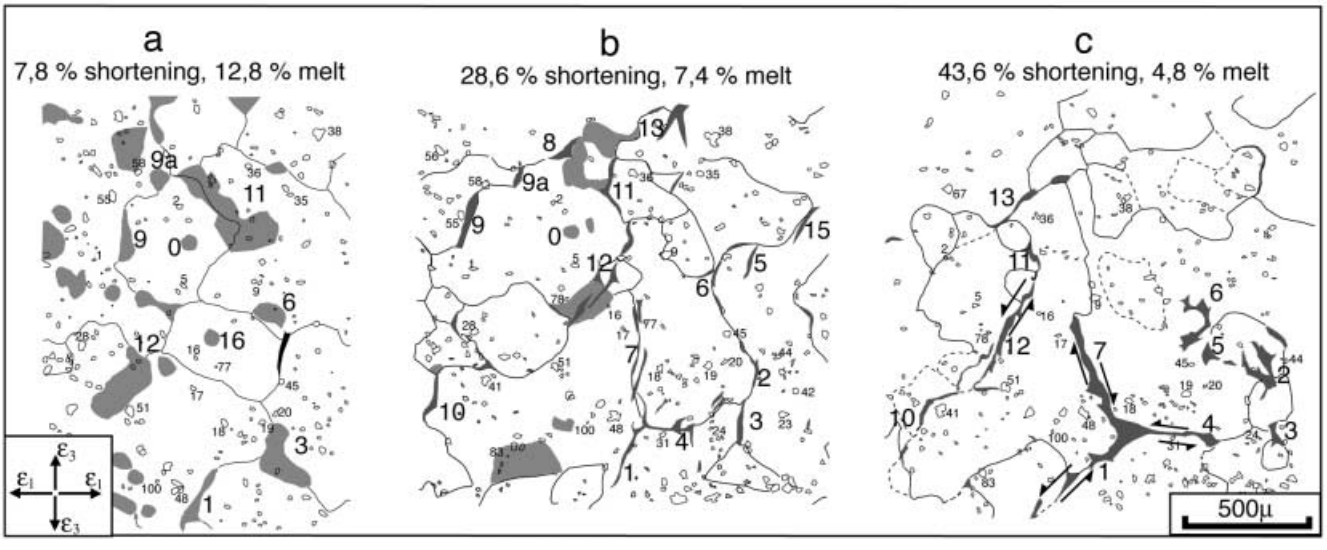

Melt topology

Grain-scale melt distribution, or topology, is a potential tool to reconstruct synkinematic transport channels, but it also helps us to understand deformation mechanisms in partially molten rocks (e.g., Bai et al. 1997) and large-scale segregation pathways (e.g., Daines and Kohlstedt 1997). Moreover, the strength of partially melted rocks can vary as a function of melt distribution (e.g., Cooper and Kohlstedt 1984). Melt distribution may be controlled by surface energy (e.g., Cooper and Kohlstedt 1984), by the magnitude and orientation of the applied differential stress (e.g., Daines and Kohlstedt 1997; Zimmerman et al. 1999), or by finite strain (e.g., Kohlstedt and Zimmerman 1996).

Static conditions and textural equilibrium

Under conditions of microstructural equilibrium, the surface-energy ratio of solid-solid boundaries to solid-melt boundaries determines the dihedral angle forming between two grains and a melt. This angle, also termed wetting angle, controls melt topology. If the wetting angle is smaller than 60°, melt is distributed in an interconnected network of grain-boundary channels. In contrast, if the wetting angle is larger than 60°, melt forms isolated pockets at grain-boundary triple junctions (see the review by Laporte et al. 1997). Experimental studies and numerical modeling of equilibrium melt distribution under static conditions in the granitic system (Laporte et al. 1997) indicate that wetting angles are generally small; a granitic melt forms dihedral angles of 22°–23° in monomineralic quartz aggregates, and 44° in a monomineralic alkali-feldspar aggregate. Laporte et al. (1997) noted that melt films may be very thin (0.3 μm) and calculated that melt percentages as small as 0.04 vol% were sufficient to form an interconnected network of melt channels throughout a quartz aggregate.

Static conditions and textural disequilibrium

If grain growth during crystallization or grain consumption during melting is faster than the rate of grain shape readjustment driven by surface energy minimization, textural equilibrium will not be achieved, and melt topology will not be controlled by the equilibrium melt-solid-solid dihedral angle. Under these conditions melt distribution will be different in crystallizing and melting aggregates (Vigneresse et al. 1996). Melt topology during melting is controlled by the distribution of mineral phases that are involved in the melting reaction. Melt forms along the phase boundaries of these grains (Mehnert et al. 1973). In contrast, if crystallization occurs under conditions of textural disequilibrium, then melt distribution is controlled by the porosity of the rock, which in turn depends on grain shapes and grain orientations.

Dynamic conditions

During deformation, melt distribution may depart from the equilibrium geometry discussed above, as shown by experimental deformation of partially molten mantle rocks (Daines and Kohlstedt 1997, for review). Experiments on deformed partially molten granites show the following melt topologies:

1. In the cataclastic flow regime experiments indicate that melt distributes along microfractures and grain boundaries oriented subparallel to the maximum compressive principal stress (van der Molen and Paterson 1979; Paquet and François 1980; Rutter and Neumann 1995), and also within microfaults which form at ~30° to the principal stress direction (van der Molen and Paterson 1979; Paquet and François 1980; Paquet et al. 1981; Rutter and Neumann 1995). These fault zones generally contain higher melt fractions than the sample as a whole, and thus enhance channeling of melt flow. For melt fractions >0.1 the preferred orientation of faults becomes weaker, and melt distribution more isotropic (Rutter and Neumann 1995).
2. In the dislocation creep regime (Dell'Angelo and Tullis 1988; Gleason et al. 1999) melt distribution varies as a function of the flow stress. Samples deformed at differential stresses higher than 100 MPa (Dell'Angelo et al. 1987) or 160 MPa (Gleason et al. 1999) exhibit intergranular melt pockets oriented parallel to the greatest principal stress direction. Increasing melt fraction (up to 0.15) enhances cataclasis (Dell'Angelo and Tullis 1988), and hence melt accumulation within axial cracks. At differential stresses lower than 100 MPa (Dell'Angelo et al. 1987) or 150 MPa (Gleason et al. 1999) melt occurs primarily at grain triple junctions and no shape preferred orientation (SPO) of the melt pockets occurs, whatever the intensity of deformation.
3. In the diffusion creep regime, samples deformed in the presence of 3 to 5% melt at flow stresses below 100 MPa show the same microstructures as for samples described above that were deformed in the dislocation creep regime at low differential stresses (Dell'Angelo et al. 1987). This result was confirmed by the experiments of Dimanov et al. (1998) on partially molten labradorite.

The latter results suggest that melt distribution in granite is controlled by differential stress rather than by deformation mechanisms, as already shown for mantle rocks (Daines and Kohlstedt 1997). Moreover, these results confirm the observations of Daines and Kohlstedt (1997) who noted that melt distribution in olivine aggregates is nearly isotropic for differential stresses lower than 100 MPa, while it is distributed

along grain boundaries oriented at an angle of 10–15° to the maximum shortening direction at stresses >100 MPa. Note however, that new experiments (M.E. Zimmerman, personal communication) on very fine grained olivine aggregates (<5 μm) show that an SPO of melt pockets can occur even if stresses are lower than 5–10 MPa.

On the basis of the small angle existing between melt pockets and principal shortening direction, Daines and Kohlstedt (1997) suggested that large-scale flow in the mantle may occur in a direction subparallel to σ_1. However, the experiments of Dell'Angelo and Tullis (1988) and Rosenberg and Handy (in review) show that the bulk flow direction of melt does not necessarily reflect the SPO of intergranular melt pockets. In these experiments, melt accumulated at both sides of the sample in the barreled parts of the sample, i.e., at sites that are incompatible with a bulk flow direction of melt subparallel to σ_1. Therefore, it was suggested that melt may flow along grain boundaries perpendicular to the shortening direction, despite the widespread occurrence of melt-bearing axial cracks.

Flow laws

The first attempt to formulate a flow law for partially molten granite was made by Rutter and Neumann (1995), based on their experiments at brittle conditions. Rutter (1997) pointed out that this flow law is purely empirical, and is probably not valid outside of the experimental conditions used by Rutter and Neumann (1995). In order to model the behavior of partially molten granite deforming in the diffusion-creep regime, Paterson (in press) and Rutter (1997) proposed a theoretical flow law, modified from Paterson (1995) for granular flow in the presence of a fluid phase. For an open system allowing melt segregation, this flow law is written as follows (Paterson, in press):

$$\dot{\varepsilon}_1 \approx \frac{8}{3}\frac{v_s^2 c D_m \phi^2}{d^2 RT}(\sigma_1 - \sigma_3).$$

In the case of a closed system it is

$$\dot{\varepsilon}_1 \approx \frac{v_s^2 c D_m \phi^2}{d^2 RT}(3(\sigma_1 - \sigma_3) + (\sigma_3 - p))$$

in which c is molar solubility (mol m^{-3}) of the component of the solid in the melt, d is the grain diameter, D_m is the diffusion coefficient of the component of the solid in the melt, ϕ is the melt fraction, m is the melt fraction exponent, and its value is 2, p is the melt pressure, R is the gas constant, σ_1 is the maximum principal stress component, σ_3 is the least principal stress component, T is the temperature, and v_s is molar internal volume of the component in the solid grain

The latter flow law was experimentally tested by Mecklenburg and Rutter (1999) in the diffusion-creep regime. The agreement between theory and experiment was good at laboratory strain rates less than ~10^{-7} s^{-1}, but not at higher strain rates.

Deformation of partially molten granite under natural conditions

A major difficulty associated with microstructural investigations of naturally deformed anatectic rocks is the poor preservation of synmagmatic microstructures. Several processes combine to obliterate the synmagmatic microstructures: (1) deformation may continue below the solidus, so that solid-state fabrics overprint magmatic fabrics. (2) Persisting high-temperature conditions may rearrange grain boundaries. In addition, because criteria to identify deformation in the presence of low melt fractions (<0.2) are poorly defined, and corresponding microstructures may resemble those of rocks deformed under high-temperature, solid-state conditions, synmagmatic microstructures may not be recognized as such. These difficulties may explain the small number of investigations concerning the microstructures of deformed partially molten granitic rocks. In the following, I review the investigated case studies in which synmagmatic deformation mechanisms were inferred. I will use the term solid-state in its strict sense, i. e., when no melt is present, and the term synmagmatic in a broad sense, i.e., for the presence of melt, irrespective of the melt fraction.

Deformation mechanisms

Fracturing

Many authors (Paquet et al. 1981; Hibbard and Watters 1985; Gapais and Barbarin 1986; Hibbard 1987; Bouchez et al. 1992; Davidson et al. 1996) described microstructural evidence for grain-scale intragranular fracturing in the presence of melt. This interpretation rests on the occurrence of fractures filled by at least one phase that is inferred to crystallize from a residual melt (Fig. 7). Bouchez et al. (1992) suggested that these structures form when the melt content is in the 10–30% range.

Widespread melt-bearing intergranular fractures were also reported (Rosenberg and Riller 2000) from a synmagmatically deformed orthogneiss. The interpretation of these structures is based on the occurrence of intergranular K-feldspar and plagioclase films preferentially distributed along grain boundaries oriented at a high angle to the foliation plane. The identification of such structures is often ambiguous, because no markers such as twin planes or grain boundaries are offset. However, intergranular fractures are expected to be common in partially molten systems, since failure under high homologous temperatures and

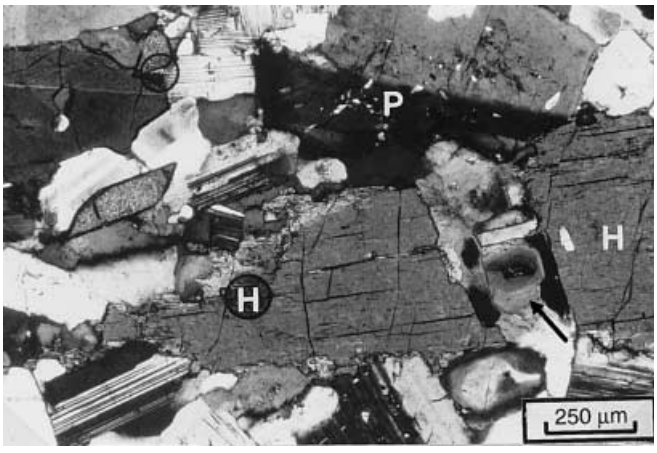

Fig. 7 Micrograph (crossed polarizers) of a synmagmatic fracture within a hornblende grain of a tonalite (Adamello pluton, Southern Alps, Italy). The *arrow* points to a euhedrally-zoned plagioclase that is inferred to have grown in the fracture from the tonalitic melt. *H* Hornblende, *P* plagioclase

low stresses is always by intergranular creep fracture (Gandhi and Ashby 1979).

In the aforementioned investigations, synmagmatic intragranular fractures affect large feldspar grains, more rarely amphibole, and never quartz or biotite. This observation suggests that (1) the strength contrast existing in the solid state between quartz and feldspar may persist into the supersolidus field; (2) fracturing in the presence of melt is an accommodating deformation mechanism, but not the dominant one; and (3) synmagmatic fractures are often preserved in nature. As a consequence, the lack of documented case studies of synmagmatic cataclastic flow in granites is not due to the poor preservation of synmagmatic microfractures. Synmagmatic cataclastic flow, as observed in many experimental investigations is therefore considered to be absent under natural conditions.

Intracrystalline plasticity

Intracrystalline plastic flow of the solid matrix during deformation of partially molten granite may be rate-competitive with melt-assisted diffusion creep only at low temperatures and high stress levels (Rutter 1997). This conclusion is based on the extrapolation of flow laws of partially molten granite and of melt-free quartz aggregates at temperatures, grain sizes and strain rates assumed to occur under natural conditions (see Fig. 4.5 in Rutter 1997). However, crystal-plastic deformation of quartz inferred to occur during flow of partially molten granite is reported several times in the literature. Gapais and Barbarin (1986) were the first to suggest the occurrence of synmagmatic dynamic recrystallization of quartz. Rosenberg and Riller (2000) inferred that intracrystalline plasticity of quartz assisted by dynamic recrystallization was the dominant deformation mechanism in a partially molten orthogneiss. In this rock, quartz grains within ribbons exhibit deformation bands and lobate grain-boundaries (Fig. 8a). Some of these grain-boundaries are coated by 5–50 μm-thick feldspar films (Fig. 8a) of plagioclase and orthoclase composition, interpreted to mimic melt topology. Occasionally, such feldspar films transect the quartz grains whose deformation features, such as deformation bands, suggest that melt intruded into a plastically deforming quartz grain.

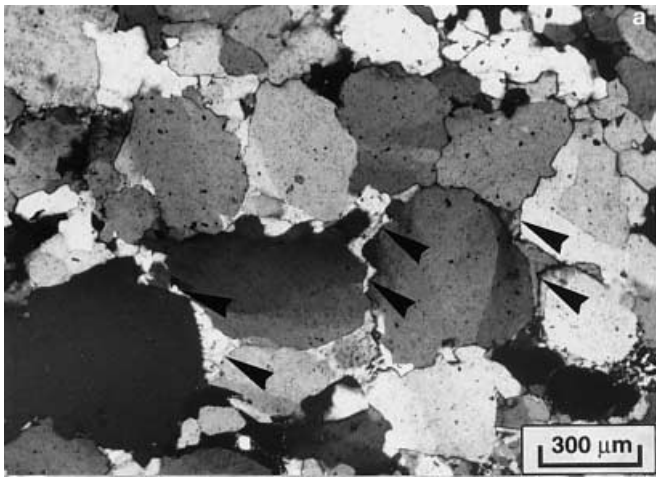

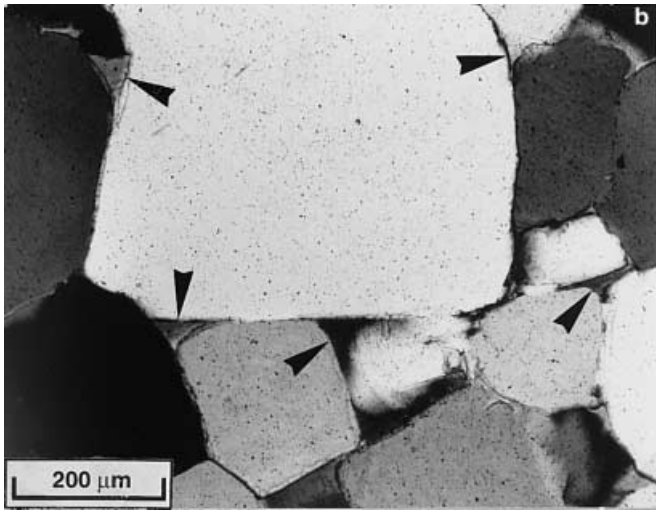

Fig. 8a,b Micrographs (crossed polarizers) of partially molten granite from the Murray Pluton (Central Ontario, Canada). **a** Quartz ribbon dynamically recrystallized in the presence of melt. *Arrowheads* point to feldspar seams along quartz grain boundaries that mimic melt topology. Note lobate grain boundaries and preferred orientation of feldspar seams subperpendicular to horizontal foliation. **b** Quartz aggregate lacking any evidence for deformation. *Arrow heads* point to intergranular feldspar seams that mimic distribution of partial melt. Note the relatively small (always <60°) dihedral angles between quartz, quartz, and feldspar, suggesting that partial melt was interconnected along grain-edge channels

Grain boundary sliding, diffusion creep and contact melting

Grain- and phase-boundary sliding may be the dominant deformation mechanism at low melt fractions, but there are few if any unambiguous diagnostic microstructures for this mechanism. An excellent example of melt-assisted grain-boundary sliding was reported by Nicolas and Ildefonse (1996) from a gabbro (Fig. 5a). Deformation was inferred to occur in the presence of ~20% melt by dissolution-accommodated sliding of grains along melt films. This process is similar to the contact melting coined by Park and Means (1996). There is no evidence for intracrystalline plasticity in these rocks. Similar microstructures are also observed in granitic rocks, as shown in Fig. 9.

Diffusion-accommodated grain- and phase-boundary sliding was inferred to occur during the last stages of crystallization of tonalitic rocks (Möbus and Rosenberg 1999). These tonalites exhibit quartz aggregates with axial ratios of ~2:1 and lobate grain boundaries (Fig. 10), indicating dynamic recrystallization. The c-axes of these grains are oriented at low angles to the stretching lineation. In contrast, the magmatic matrix surrounding these quartz aggregates does not show any evidence of crystal-plastic deformation (Fig. 10). However, the strain undergone by the quartz aggregates must also have affected the surrounding matrix, since the quartz aggregates do not form interconnected layers. Such a "cryptic" deformation on the grain scale is therefore ascribed to diffusion-accommodated grain-boundary sliding. The large grain size of these tonalites (>0.5 mm) and the euhedral shape of all grains surrounding the quartz aggregates most likely preclude deformation under subsolidus conditions. Therefore, the plagioclase-dominated matrix of these tonalites likely deformed by dissolution-accommodated grain-boundary sliding in the presence of melt.

Fig. 9 Micrograph (crossed polarizers) of a tonalite from the Adamello Pluton (Southern Alps, Italy). Note the indentations (*arrows*) of plagioclase grains into each other, cross-cutting the euhedral zonation rims. Indentations are inferred to result from dissolution at grain-to-grain contacts in the presence of melt

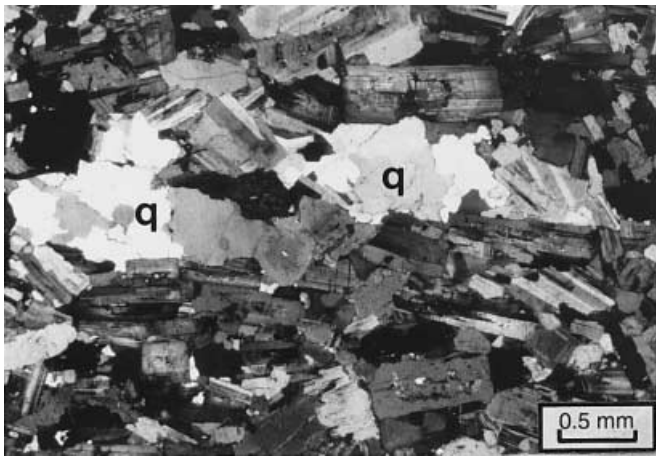

Fig. 10 Micrograph (crossed polarizers) of tonalite from the Adamello Pluton (Southern Alps, Italy). *q* Quartz aggregates elongate parallel to the foliation plane. Lobate boundaries of quartz grains suggest dynamic recrystallization. In contrast, the matrix surrounding the quartz aggregates consists of euhedral grains of plagioclase, some hornblende, and minor biotite

A melt-induced transition from dislocation creep to diffusion creep, as previously found in experiments, were inferred to occur in nature (Rosenberg and Berger in press) in partially molten orthogneisses. The microstructures of the restitic parts of these orthogneisses are indicative of dislocation creep, whereas the leucosome in these rocks shows microstructures indicative of diffusion-accommodated grain-boundary sliding in the presence of melt.

Melt topology

Preservation of melt topology at the outcrop-scale and sample-scale is common in the form of leucosome veins in migmatites (e.g., Brown et al. 1999). In contrast, the preservation of grain-scale melt topology in deep-seated crustal rocks is rare. When preserved, melt topology is inferred from the distribution of glass in quenched xenoliths (e.g., Cesare et al. 1997) or from the distribution of mineral phases assumed to mimic residual melt topology (e.g., Brown et al. 1999; Holness and Clemens 1999; Rosenberg and Riller 2000; Sawyer 2000).

Under static conditions, suggested by the absence of microstructural evidence for deformation, the dihedral angles between the inferred granitic melt (outlined by interstitial feldspar in Fig. 8b) and the quartz grains are smaller than 60° (Holness and Clemens 1999; Rosenberg and Riller 2000). This suggests that melt forms interconnected grain-boundary channels within quartz aggregates, in agreement with the crystallization experiments on synthetic granitic compositions (e.g., Laporte et al. 1997). Deformation induces

a change from isotropic melt pockets at triple grain junctions, to elongate pockets preferentially oriented subperpendicular to the foliation plane (Fig. 8a; Rosenberg and Riller 2000). This orientation of the melt pockets agrees with what is observed in partially molten rocks experimentally deformed at high (>100–150 MPa) differential stresses, provided that the maximum compressive stress is assumed to form a high angle to the foliation plane. However, the latter example may be an exception and not the rule. More often, melt films and pockets in natural granites are preferentially located along grain boundaries parallel to the foliation plane (Sawyer 1999, in press; Rosenberg and Berger in press). The latter studies show that the long axes of melt pockets exhibit two maxima: the largest maximum is oriented parallel to the foliation plane, whereas the smaller maximum is subperpendicular to the foliation. Moreover, melt films parallel to the foliation are longer than those perpendicular to the foliation. Assuming that the shortening direction was at a high angle to the foliation plane, the spatial distribution of melt pockets described above is in contrast with that observed under experimental conditions. The same discrepancy exists in mantle rocks, which often preserve evidence for foliation-parallel interstitial melt (Jousselin and Mainprice 1999; Lamoureux et al. 1999) in contrast with experimentally deformed olivine aggregates.

Another important observation in the studies of Sawyer (1999) and Rosenberg and Berger (in press) is the film-like distribution of melt along grain boundaries during crystallization. Such melt distribution differs from that expected by static percolation models (Vigneresse et al. 1996) for crystallization. More examples of preserved syntectonic melt topology from natural rocks are needed for a general statement to be made about the grain-scale relationship between melt pockets and kinematic axes.

Criteria for the identification of synmagmatic deformation in natural rocks

Microstructural criteria for the identification of deformation in the presence of melt have been discussed by many authors (Hibbard and Watters 1985; Gapais and Barbarin 1986; Hibbard 1987; Blumenfeld and Bouchez 1988; Hutton 1988; Paterson et al. 1989; Nicolas 1992; Tribe and D'Lemos 1996; Paterson et al. 1998; Sawyer 1999). These authors tentatively correlate specific microstructures and deformation mechanisms with specific ranges of melt fractions.

Deformation in the presence of melt can be divided into three types of flow (Gapais and Barbarin 1986; Hibbard 1987; Wickham 1987; Paterson et al. 1989; Nicolas 1992; Paterson and Tobisch 1992), corresponding to melt fractions higher than the RCMP, equal to the RCMP, and lower than the RCMP. However, within these three ranges of melt fractions, the rheology and probably the microstructure of rock will certainly vary as a function of the melt fraction, as shown by Hirth and Kohlstedt (1995a, 1995b). Keeping this in mind, the above mentioned classification is a good starting point to describe synmagmatic foliations. In accordance with Paterson et al. (1989) and Gapais and Barbarin (1986), the term "magmatic state" will be used for deformation at melt fractions above 0.45; after Paterson et al. (1989) the term "submagmatic" will be used for deformation at melt fractions between 0.45 and 0.2. At still lower melt fractions the terms "deformation at low melt fractions" will be preferred to the "high-temperature solid-state" of Paterson et al. (1989), in order to better distinguish solid-state deformation under melt-absent and melt-present conditions.

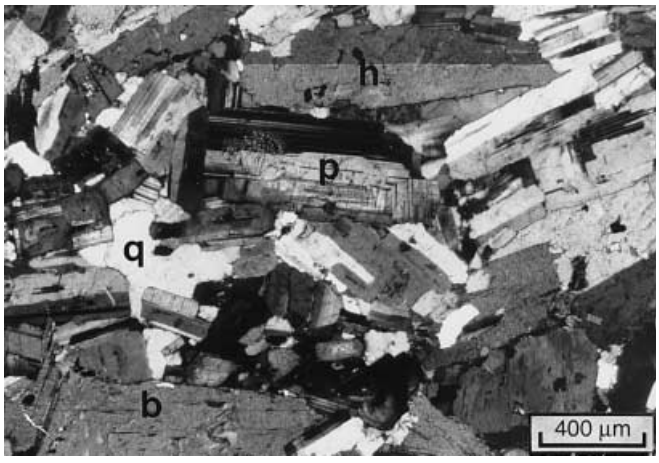

Fig. 11 Micrograph (crossed polarizers) of a magmatically foliated tonalite from the Adamello Pluton (Southern Alps, Italy). Note the shape preferred orientation (*SPO*) of all grains and the lack of crystal plastic deformation. *p* Plagioclase, *q* quartz, *h* hornblende, *b* biotite

Magmatic flow

Foliations resulting from magmatic flow are expected to form by the passive rotation of anisometric grains within the melt. A magmatic foliation is characterised by the planar SPO of magmatic grains that do not show any evidence of crystal-plastic deformation (Fig. 11). Rocks preserving a magmatic foliation in the strict sense are inferred to have undergone flow at high melt fractions (>0.45) and subsequent crystallization under static conditions. In the analogue experiments of Park and Means (1996), however, such foliations formed at melt fractions as low as 0.1[1].

[1] The melt fraction was not mentioned by Park and Means (1996). I estimated the "local" melt fraction (not the one of the bulk sample) by calculating the surface area of melt in their Fig. 4a, b, using the program NIH Image (Rasband 1997).

Tikoff and Teyssier (1994) and Tribe and D'Lemos (1996) suggested that the occurrence of tiling, i.e., the imbrication of clasts due to rigid body rotation in a molten matrix (Fernandez et al. 1983) may reflect the transition from magmatic flow to submagmatic flow (defined as post-RCMP by Tribe and D'Lemos 1996). This is not supported, however, by the analogue experiments of Arbaret et al. (1996) and Fernandez and Fernandez-Catuxo (1997), in which tiling occurs even at melt fractions higher than 0.6. In summary, magmatic foliations certainly develop in the presence of melt, but do not define a specific interval in the melt fraction.

Submagmatic flow (20–50% melt)

Flow in the submagmatic state is characterized by grain-to-grain interaction and a reduced ability of the grains to rotate freely in the melt, compared with the magmatic state. Analogue experiments showed that grain-to-grain interactions tend to rotate the particles towards a stable end orientation, coinciding with the flow plane (see Ildefonse et al. 1997). Flow in the submagmatic state is therefore expected to develop a foliation parallel to the flow plane more readily than in the magmatic state. Foliations resulting from submagmatic flow may show some fracturing and/or crystal-plastic behavior of grains in response to the increasingly frequent grain-to-grain interactions. As discussed above, however, magmatic foliations may persist in the submagmatic state. The critical parameter controlling the onset of crystal-plasticity is probably the strain rate. Park and Means (1996) showed in their experiments that fast strain rates (10^{-4} s^{-1}) induce crystal-plastic deformation, thus destroying the euhedral shape of the grains, even at melt fractions as high as 0.27[2]. In contrast magmatic foliations persist at melt fractions of 0.1 when the strain rate is slow (3×10^{-5} to 3×10^{-6} s^{-1}). Therefore, provided a solid framework has formed and the melt fraction is lower than ~0.3, it is the strain rate rather than the melt fraction which determines the microstructure of the deforming partially molten rock.

In conclusion, synmagmatic fracturing, dynamic recrystallization, and contact melting are diagnostic of mechanical interactions between grains at melt fractions <0.5. Conversely, the absence of these features does not allow one to constrain the melt fraction, as shown by the low strain rate experiments of Park and Means (1996).

[2] The melt fraction was estimated as in footnote 1, from Fig. 2a of Park and Means (1996).

Flow at low (<20% melt) melt fractions

Rocks deformed in the presence of low (<0.2) melt fractions may develop microstructures very similar to those acquired at high-temperature, subsolidus conditions. Therefore, criteria to distinguish these two types of flow are often lacking. In this regard, it is interesting to note that melt is never mentioned in any of the terms used so far to define flow in the presence of melt fractions <0.2: "crystal-plastic strain" (Hutton 1988), "high-temperature, solid-state flow" (Paterson et al. 1989), "solid-state creep" (Cruden 1990), and "solid-state flow" (Nicolas 1992).

Even in the few studies which do infer the occurrence of low melt fractions during deformation, the estimate of melt volume is generally poorly constrained. For example, Gapais and Barbarin (1986) suggested that during the last stages of granite crystallization, crystal-plastic deformation of quartz occurred in the presence of a melt fraction up to the RCMP (see their Fig. 8). However, both their observed microstructures and crystallographic preferred orientation (CPO) in quartz are also observed under high-temperature, subsolidus conditions (e.g., Schmid et al. 1981). Therefore, neither the CPO nor the microstructure of quartz can be used to distinguish subsolidus from hypersolidus conditions.

In the study of Rosenberg and Riller (2000), the melt content is estimated through the volume proportion of interstitial feldspar films enclosed in the quartz ribbons, assumed to represent ~0.5 of the granitic melt. Quartz microstructures in these rocks do not differ from those observed under high-temperature, solid-state conditions. It is only the preservation of interstitial films that mimic melt that allows one to infer synmagmatic deformation at low melt fractions.

Hibbard (1987) and Bouchez et al. (1992) describe synmagmatic fractures that were inferred to form at melt fractions of up to 0.3. Bouchez et al. (1992) provide several criteria to distinguish such fractures from those formed in the solid state: (1) presence of magmatic minerals filling the fractures. For example the An content of a plagioclase filling a fracture is expected to be closer to the minimum melt composition than in other locations; (2) fractures transecting single grains; (3) quartz within a fracture must be in crystallographic continuity with quartz outside of the fracture. Hibbard (1987) suggested that deformation of plutonic rocks in the presence of 10% melt can be identified by "fluid relocation textures" or low-pressure sites into which late-stage hydrous melts are inferred to migrate. Crystallization within pressure shadows (see also Gapais and Barbarin 1986) of K-feldspar and plagioclase with lower Ba and lower An contents, respectively, than the feldspar clast is attributed to late stage crystallization from the melt. Note, however, that compositional differences between grains crystallized from partial or residual

melts and grains of the unmelted matrix are rarely preserved in nature (e.g., Ashworth 1985).

In the study by Nicolas and Ildefonse (1996), the presence of 20% melt in the deforming gabbro is inferred indirectly from seismic data on magma chambers in the mantle. Indentations between euhedral grains (Figs. 5a and 9) in the absence of crystal-plastic deformation may be a good indicator for deformation in the presence of low melt fractions.

Deformation of a quartz analogue (norcamphor) by dislocation creep involving dynamic recrystallization in the presence of less than 20% melt (Rosenberg and Handy, submitted) yields at most a very weak SPO of the solid grains. In contrast, under dry conditions, at the same temperature and deformation rates, the same material develops a strong SPO parallel to the principal stretching direction. Hirth and Kohlstedt (1995b) also observed this behaviour in partially molten olivine aggregates. These observations may be diagnostic of deformation in the presence of low melt fractions in a rock undergoing dynamic recrystallization.

In summary, there are good microstructural criteria to identify synmagmatic fracturing (Bouchez et al. 1992) and contact melting (Nicolas and Ildefonse 1996). These allow one to distinguish subsolidus and hypersolidus conditions. In contrast, if deformation at low melt fractions occurred by intracrystalline plasticity, there are few if any microstructural criteria that allow one to determine whether melt was present or not during deformation. Quantification of melt fractions in the range between 0 and 0.2 remains speculative.

Conclusions

1. Whether or not melt fraction vs. log. strength (or viscosity) curves do show a sigmoid shape indicating the existence of an RCMP depends on the experimental conditions. If melt viscosity is low (e.g., $10^{4.5}$ Pa s), an RCMP is present for laboratory strain rates in the order of 10^{-5} s^{-1}. In nature, melt viscosities are inferred to be low ($10^{4.5}$ Pa s, Scaillet et al. 1998). In addition, a major rheological threshold at melt fractions of 0.4 (i.e., close to the RCMP), may be inferred from volcanic rocks. Therefore, an RCMP probably occurs under natural conditions.
2. Investigations of natural samples show that both diffusion-accommodated grain boundary sliding and dislocation creep involving dynamic recrystallization do occur at melt fractions below 0.2. Grain boundary sliding was documented in gabbros at grain sizes larger than 1 mm and in tonalites at grain sizes larger than 0.5 mm. Except for pseudotachylites, cataclastic flow in partially molten crustal rocks has not been observed in nature. Therefore, most experimental results on the deformation of partially molten granites do not adequately reproduce natural conditions.
3. Melt topology under experimental conditions is controlled by the orientation of the principal stress directions if the differential stresses are high (>100–150 MPa). Under these conditions, melt distribution clearly deviates from the equilibrium geometry observed under static conditions. Irrespective of melting or crystallization conditions, melt pockets are expected to be oriented at 0 to 30° from the principal compressive stress direction. Therefore, under these conditions, permeability thresholds for crystallizing and melting rocks do not differ.

   In contrast, at low differential stresses under both static and dynamic conditions, melt topology is governed by surface energy. Melt pockets do not have a preferred orientation, and their shape is dictated by the wetting angles of mineral pairs and melt, and by the anisotropic crystallography of the minerals. Under these conditions, melt distribution in melting rocks may differ from that in crystallizing rocks. Wetting of grain boundaries may be more effective during melting, because melt films form along the entire phase boundaries of those minerals involved in the melting reaction. Such melt distribution favors diffusion creep and grain boundary sliding.

   The relationship between the bulk flow direction of melt and the orientation of intergranular melt pockets is not straightforward. The orientation of grain-scale melt pockets does not simply reflect the dominant flow direction of melt through the rock. More experiments on aggregates in which segregation occurs during deformation need to be performed.
4. Microstructural criteria cannot always be used to estimate melt fractions at the time of deformation. Foliations formed by the alignment of magmatic euhedral grains do not reflect a specific range of melt fractions, because they can form over a wide crystallization interval from the magmatic state down to melt fractions of 0.1. At low melt fractions (<0.2) and in rocks deformed in the dislocation creep regime, microstructural criteria to distinguish subsolidus from hypersolidus conditions are generally lacking. If fracturing or contact melting affected the partially molten granites, microstructural evidence for deformation in the presence of melt may be easier to detect.
5. Many factors controlling the rheology of partially molten rocks that are known to occur in nature have not yet been reproduced in experimental studies: (a) segregation processes and the effect of different rates of melting on deformation and segregation. Drained experiments are needed to reproduce such conditions; (b) the effect of mechanical anisotropies such as foliations formed by micas or compositional layering. These anisotro-

pies may be the cause of the commonly observed melt pockets (leucosomes) parallel to the flattening plane in migmatitic rocks. Such melt distribution has not been observed in experiments yet; (c) flow laws derived from experiments performed in the diffusion creep regime and dislocation creep regime are needed to model the rheology of the partially molten crust. Experimental work is in progress (Mecklenburg and Rutter 1999) to test a theoretical flow law for the diffusion creep regime, but no data exist for the dislocation creep regime; (d) although the mechanical behavior of quartz and feldspar at high temperature is better understood than that of micas and aluminosilicates, granites are not necessarily representative of middle crustal rocks undergoing large-scale anatexis. Deformation experiments on metapelites and metapsammites are needed to constrain the rheology of partially molten crustal sections.

Acknowledgements Jean Luc Bouchez, Mike Brown, Mark Handy, and Jörg Renner provided very helpful reviews. A. Berger and M. Handy shared many discussions on the subject of deformation of partially molten rocks. I am grateful to M.S. Paterson for a preprint of his work. Jörg Renner and Ed Sawyer are thanked for showing me their unreviewed manuscripts, and Mark Zimmerman for discussing his unpublished experimental results. C. Möbus and M. Rosenau helped to prepare the figures. Grants by the DFG ("Orogene Prozesse...", HA 2403/2, and RO 2177/1) are kindly acknowledged.

References

Arbaret L, Diot H, Bouchez JL (1996) Shape fabrics of particles in low concentration suspensions: 2D analogue experiments and application to tiling in magma. J Struct Geol 18:941–950

Arzi AA (1978) Critical phenomena in the rheology of partially melted rocks. Tectonophysics 44:173–184

Ashworth JR (1985) Introduction. In: Ashworth JR (ed) Migmatites. Blackie, Glasgow, pp 1–31

Auer F, Berckhemer H, Oehlschlegel G (1981) Steady state creep of fine grain granite aggregate at partial melting. J Geophys 49:89–92

Bagdassarov N, Dorfman A (1998) Granite rheology: magma flow and melt migration. J Geol Soc Lond 155:863–872

Bai Q, Jin Z-M, Green W II (1997) Experimental investigation of the rheology of partially molten peridotite at upper mantle pressures and temperatures. In: Holness MB (ed) Deformation-enhanced fluid transport in the Earth's crust and mantle. The Mineralogical Society Series, 8. Chapman & Hall, London, pp 40–61

Barboza S, Bergantz G (1998) Rheological transitions and the progress of melting of crustal rocks. Earth Planet Sci Lett 158:19–29

Berger A, Kalt A (1999) Structures and melt fractions as indicators of rheology in cordierite-bearing migmatites of the Bayerische Wald (Variscan Belt, Germany). J Petrol 40:1699–1719

Blumenfeld P, Bouchez JL (1988) Shear criteria in granite and migmatite deformed in the magmatic and solid states. J Struct Geol 10:361–372

Bouchez JL, Delas C, Gleizes G, Nédélec A, Cuney M (1992) Submagmatic fractures in granites. Geology 20:35–38

Brace WF, Martin RJ (1968) A test of the low of effective stress for crystalline rocks of low porosity. Int J Rock Mech Min Sci 5:415–426

Brown M, Rushmer T (1997) The role of deformation in the movement of granitic melt: views from the laboratory and the field. In: Holness MB (ed) Deformation-enhanced fluid transport in the Earth's crust and mantle. The Mineralogical Society Series, 8. Chapman & Hall, London, pp 111–144.

Brown MA, Brown M, Carlson WD, Denison C (1999) Topology of syntectonic melt flow networks in the deep crust: inferences from three-dimensional images of leucosome geometry in migmatites. Am Mineral 84:11–12, 1793–1818

Cesare B, Salvioli Mariani E, Venturelli G (1997) Crustal anatexis and melt extraction during deformation in the restitic xenoliths at El Joyazo (SE Spain). Min Mag 61:15–27

Clemens JD, Petford N (1999) Granitic melt viscosity and silicic magma dynamics in contrasting tectonic settings. J Geol Soc Lond 156:1057–1060

Cooper RF, Kohlstedt DL (1984) Solution-precipitation enhanced diffusional creep of partially molten olivine-basalt aggregates during hot-pressing. Tectonophysics 107:207–233

Cruden AR (1990) Flow and fabric development during the diapiric rise of magma. J Geol 98:681–698

Daines MJ, Kohlstedt DL (1997) Influence of deformation on melt topology in peridotites. J Geophys Res 102:10257–10271

Davidson C, Hollister LS, Schmid SM (1992) Role of melt in the formation of a deep-crustal compressive shear zone: the MacLaren Glacier metamorphic belt, south central Alaska. Tectonics 11:348–359

Davidson C, Rosenberg CL, Schmid SM (1996) Synmagmatic folding of the base of the Bergell pluton: evidence from the western contact. Tectonophysics 265:213–238

Dell'Angelo LN, Tullis J (1988) Experimental deformation of partially melted granitic aggregates. J Metamorph Geol 6:495–515

Dell'Angelo LN, Tullis J, Yund RA (1987) Transition from dislocation creep to melt-enhanced diffusion creep in fine-grained granitic aggregates. Tectonophysics 139:325–332

Dimanov A, Dresen G, Wirth R (1998) High-temperature creep of partially molten plagioclase aggregates. J Geophys Res 103:9651–9664

Fernandez A, Gasquet DR (1994) Relative rheological evolution of chemically contrasted coeval magmas: example of the Tichka plutonic complex (Morocco). Contrib Mineral Petrol 116:316–326

Fernandez A, Fernandez-Catuxo J (1997) 3D biotite shape fabric experiments under simple shear strain. In: Bouchez JL, Hutton DHW, Stephens WE (eds) Granite: from segregation of melt to emplacement fabrics. Kluwer, Dordrecht, pp 145–157

Fernandez A, Feybesse J, Mezure J (1983) Theoretical and experimental study of fabrics developed by different shaped markers in two dimensional simple shear. Bull Soc Geol Fr 3:319–326

Gandhi C, Ashby MF (1979) Fracture-mechanism maps for materials which cleave: F.C.C., B.C.C. and H.C.P. metals and ceramics. Acta Metall 27:1565–1602

Gapais D, Barbarin B (1986) Quartz fabric transition in a cooling syntectonic granite (Hermitage, France). Tectonophysics125:357–370

Gleason GC, Bruce V, Green HW (1999) Experimental investigation of melt topology in partially melted quartzo-feldspathic aggregates under hydrostatic and non-hydrostatic stress. J Metamorph Geol 17:705–722

Handy MR (1990) The exhumation of cross sections of the continental crust: structure, kinematics and rheology. In: Salisbury MH, Fountain DM (eds) Exposed cross sections of the continental crust. Kluwer, Dordrecht, pp 485–507

Hibbard MJ (1987) Deformation of incompletely crystallized magma systems: granitic gneisses and their tectonic implications. J Geol 95:543–561

Hibbard MJ, Watters RJ (1985) Fracturing and diking in incompletely crystallized granitic plutons. Lithos 18:1–12

Hirth G, Kohlstedt DL (1995a) Experimental constraints on the dynamics of the partially molten upper mantle: deformation in the diffusion creep regime. J Geophys Res 100:1981–2001

Hirth G, Kohlstedt DL (1995b) Experimental constraints on the dynamics of the partially molten upper mantle 2. Deformation in the dislocation creep regime. J Geophys Res 100:15441–15449

Hollister LS, Crawford ML (1986) Melt enhanced deformation: a major tectonic process. Geology 14:558–561

Holness M, Clemens J (1999) Partial melting of the Appin Quartzite driven by fracture-controlled H_2O infiltration in the aureole of the Ballachulish Igneous Complex, Scottish Highlands. Contrib Mineral Petrol 136:154–168

Holtz F, Scaillet B, Behrens H, Schulze F, Pichavant M (1996) Water contents of felsic melts: application to the rheological properties of granitic magmas. Trans R Soc Edinb Earth Sci 87:57–64

Hutton DHW (1988) Granite emplacement mechanisms and tectonic controls: inferences from deformation studies. Trans R Soc Edinb Earth Sci 79:245–255

Ildefonse B, Arbaret L, Diot H (1997) Rigid particles in simple shear flow: is their preferred orientation periodic or steady-state? In: Bouchez JL, Hutton DHW, Stephens WE (eds) Granite: from segregation of melt to emplacement fabrics. Kluwer, Dordrecht, pp 177–185

Jin Z, Green HW, Zhou Y (1994) Melt topology in partially molten mantle peridotite during ductile deformation. Nature 372:164–167

Jeffrey DJ, Acrivos A (1976) The rheological properties of suspensions of rigid particles. Am Inst Chem Eng J 22:417–432

Jousselin D, Mainprice D (1999) Melt topology and seismic anisotropy in mantle peridotites of the Oman ophiolite. Earth Planet Sci Lett 164:553–568

Kohlstedt DL, Zimmerman ME (1996) Rheology of partially molten mantle rocks. Annu Rev Earth Planet Sci 24:41–62

Komar PD (1972) Flow differentiation in igneous dikes and sills; profiles of velocity and phenocryst concentration. Geol Soc Am Bull 83:3443–3448

Lamoureux G, Ildefonse B, Mainprice D (1999) Modelling the seismic properties of fast-spreading ridge crustal Low-Velocity Zones: insights from Oman Gabbro textures. Tectonophysics 312:283–302

Laporte D, Rapaille C, Provost A (1997) Wetting angles, equilibrium melt geometry, and the permeability threshold of partially molten crustal protholiths. In: Bouchez JL, Hutton DHW, Stephens WE (eds) Granite: from segregation of melt to emplacement fabrics. Kluwer, Dordrecht, pp 31–54

Lejeune A, Richet P (1995) Rheology of crystal-bearing silicate melts: an experimental study at high viscosities. J Geophys Res 100:4215–4229

Marsh BD (1981) On the crystallinity, probability of occurrence, and rheology of lava and magma. Contrib Mineral Petrol 78:85–98

Means WD (1989) Synkinematic microscopy of transparent polycrystals. J Struct Geol11:163–174

Mecklenburg J, Rutter EH (1999) Deformation of partially-molten synthetic granite: laboratory evidence for granular flow. Abstract volume of the meeting, Deformation mechanisms, rheology, microstructures, p 36

Mehnert KR, Büsch W, Schneider G (1973) Initial melting at grain boundaries of quartz and feldspar in gneisses and granulites. Neues Jahrb Mineral Monatsh 4:165–183

Möbus C, Rosenberg CL (1999) Which deformation mechanisms control the flow of granitoid rocks at low (<30%) melt fractions?. Cah BRGM 290:99

Murrel SAF, Chakravarty S (1973) Some new rheological experiments on igneous rocks at temperatures up to 1,120 °C. Geophys J R Astron Soc34:211–250

Murrel SAF, Ismail IAH (1976) The effect of temperature on the strength at high confining pressure of granodiorite containing free and chemically-bound water. Contrib Mineral Petrol 55:317–330

Nelson KD, Zhao W, Brown LD, Kuo J, Jinkai C, Liu X, Klemperer SL, Makovsky Y, Meissner R, Mechie J, Kind R, Wenzel F, Ni J, Nabelek J, Leshou C, Tan H, Wei W, Jones AG, Booker J, Unsworth M, Kidd WSF, Hauck M, Alsdorf D, Ross A, Cogan M, Wu C, Sandvol E, Edwards M (1996) Partially molten middle crust beneath southern Tibet: synthesis of Project INDEPTH results. Science 274:1684–1687

Nicolas A (1992) Kinematics in magmatic rocks with special reference to gabbros. J Petrol 33:891–915

Nicolas A, Ildefonse B (1996) Flow mechanism and viscosity in basaltic magma chambers. Geophys Res Lett 23:2013–2016

Paquet J, François P (1980) Experimental deformation of partially melted granitic rocks at 600–900 °C and 250 MPa confining pressure. Tectonophysics 68:131–146

Paquet J, François P, Nédélec A (1981) Effect of partial melting on rock deformation: experimental and natural evidences on rocks of granitic compositions. Tectonophysics 78:545–565

Park Y (1994) Microstructural evolution in crystal-melt systems. PhD Thesis, State University of New York at Albany

Park Y, Means WD (1996) Direct observation of deformation processes in crystal mushes. J Struct Geol 18:847–858

Park Y, Means WD (1997) Crystal rotation and growth during grain flow in a deforming crystal mush. In: Sengupta S (ed) Evolution of geological structures in micro- to macro-scales. Chapman and Hall, London, pp 245–258

Paterson MS (1995) A theory for granular flow accommodated by material transfer via an intergranular fluid. Tectonophysics 245:135–152

Paterson MS (2001) A granular flow theory for the deformation of partially melted rock. Tectonophysics (in press)

Paterson SR, Tobisch OT (1992) Rates of processes in magmatic arcs: implications for the timing and nature of pluton emplacement and wall rock deformation. J Struct Geol 14:291–300

Paterson SR, Vernon RH, Tobisch OT (1989) A review of criteria for the identification of magmatic and tectonic foliations in granitoids. J Struct Geol 11:349–363

Paterson SR, Fowler Jr TK, Schmidt KL, Yoshinobu AS, Yuan ES, Miller RB (1998) Interpreting magmatic fabric patterns in plutons. Lithos 44:53–82

Rasband W (1997) Image 1.61. National Institute of Health. Research Services Branch NIMH

Renner J, Evans B, Hirth G (2000) On the rheological critical melt fraction. Earth Planet Sci Lett 181:585–594

Roscoe R (1952) The viscosity of suspensions of rigid spheres. Br J Appl Phys 3:267–269

Rosenberg CL, Berger A (2001) Syntectonic melt pathways in granite, and melt-induced transition in deformation mechanisms. Phys Chem Earth (A) (in press)

Rosenberg CL, Handy MR (2000) Syntectonic melt pathways during simple shearing of a partially-molten rock analogue (norcamphor-benzamide). J Geophys Res 105:3135–3149

Rosenberg CL, Riller U (2000) Partial melt topology in statically and dynamically recrystallized granite. Geology 28:7–10

Rosenberg CL, Handy MR (2001) Mechanisms and orientation of melt segregation paths during pure shearing of a partially molten rock analogue (norcamphor-benzamide). J Struct Geol (in press)

Rushmer T (1996) Melt segregation in the lower crust: how have experiments helped us? Trans R Soc Edinb Earth Sci 87:73–83

Rutter EH (1997) The influence of deformation on the extraction of crustal melts: a consideration of the role of melt-assisted granular flow. In: Holness MB (ed) Deformation-enhanced fluid transport in the Earth's crust and mantle. The Mineralogical Society Series, 8. Chapman & Hall, London, pp 82–110

Rutter EH, Neumann DHK (1995) Experimental deformation of partially molten Westerly granite under fluid-absent conditions, with implications for the extraction of granitic magmas. J Geophys Res 100:15697–15715

Sawyer EW (1999) Criteria for the recognition of partial melting. Phys Chem Earth (A) 24:269–279
Sawyer EW (2000) Melt segregation in the continental crust: distribution and geometry of melt in anatectic rocks. J Metamorph Geol (in press)
Scaillet B, Holtz F, Pichavant M (1997) Rheological properties of granitic magmas in their crystallization range. In: Bouchez, JL, Hutton DHW, Stephens WE (eds) Granite: from segregation of melt to emplacement fabrics. pp 11–29
Scaillet B, Holtz F, Whittington A, Pichavant M (1998) Phase equilibrium constraints on the viscosity of silicic magmas. 1. Volcanic-plutonic comparison. J Geophys Res 103:27257–27266
Schmid SM, Casey M, Starkey J (1981) An illustration of the advantages of a complete texture analysis described by the orientation distribution function (ODF) using quartz pole figure data. Tectonophysics 78:101–117
Schmitz M, Kley J (1997) The geometry of the central Andean backarc crust: joint interpretation of cross-section balancing and seismic refraction data. J S Am Earth Sci 10:99–110
Smith JV (1997) Shear thickening dilatancy in crystal-rich flows. J Volcan Geotherm Res 79:1–8
Tikoff B, Teyssier C (1994) Strain and fabric analyses based on porphyroclast interaction. J Struct Geol 16:477–491
Tribe IR, D'Lemos RS (1996) Significance of a hiatus in down-temperature fabric development within syn-tectonic quartz diorite complexes, Channel Islands, UK. J Struct Geol 153:127–138
Urai JL (1983) Water assisted dynamic recrystallization and weakening in polycrystalline bischofite. Tectonophysics 96:125–187
Urai JL, Means WD, Lister GS (1986) Dynamic recrystallization of minerals. In: Hobbs BE, Heard HC (eds) Mineral and rock deformation: laboratory studies. Geophys Monogr 36:161–199
van der Molen I, Paterson MS (1979) Experimental deformation of partially-melted granite. Contrib Mineral Petrol 70:299–318
Vauchez A, Egydio da Silva M (1992) Termination of a continental-scale strike-slip fault in partially melted crust: the West Pernambuco shear zone, northeast Brazil. Geology 20:1007–1010
Vernon RH (2000) Review of microstructural evidence of magmatic and solid-state flow. Electronic Geosci 5:2
Vigneresse JL, Barbey P, Cuney M (1996) Rheological transitions during partial melting and crystallization with application to felsic magma segregation and transfer. J Petrol 37:1579–1600
Wada Y (1995) Reply to the comment by Kerr RC and Lister JR on "On the relationship between dike width and magma viscosity". J Geophys Res 100:15543–15544
Wickham SM (1987) The segregation and emplacement of granitic magmas. J Geol Soc Lond 144:281–297
Wyborn D, Chappel BW, Johnston RM (1981) Three S-type volcanic suites from the Lachlan Fold Belt, southeast Australia. J Geophys Res 86:10335–10348
Zimmerman ME, Zhang S, Kohlstedt DL, Karato S (1999) Melt distribution in mantle rocks deformed in shear. Geophys Res Lett 26:1505–1508